

Supporting Information

Dual-Response for Hg^{2+} and Ag^+ Ions Based on Biomimetic Funnel-Shaped Alumina Nanochannels

Huimin Wang, Shengnan Hou, Qinqin Wang, Zhiwei Wang, Xia Fan,* Jin Zhai*

Key Laboratory of Bio-Inspired Smart Interfacial Science and Technology of Ministry of Education, School of Chemistry and Environment, Beihang University, Beijing 100191, P. R. China.

*Address correspondence to: fanxia@buaa.edu.cn (Xia Fan), zhaijin@buaa.edu.cn (Jin Zhai)

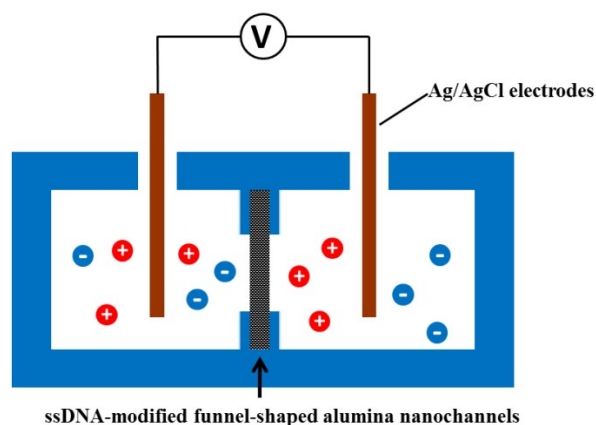


Figure S1. The experimental setup used for I-V measurement in this article.

The ionic current was measured by Keithley 6487 picoammeter/voltage source. The functional alumina nanochannels were mounted between two halves of an electrochemical cell, and each half cell was filled with 10 mM KCl, as shown in Figure S1. Ag/AgCl electrodes were settled in each half-cell to apply a transmembrane potential across the nanochannels. The currents of the ssDNA-modified alumina nanochannels under the condition of absence and presence of Hg^{2+} or Ag^+ ions were measured.

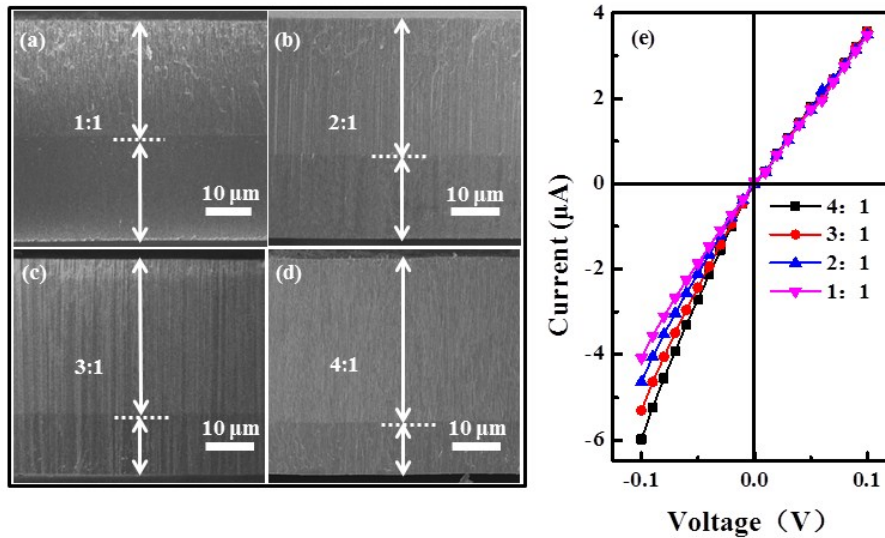


Figure S2. The cross-section viewing of the funnel-shaped alumina nanochannels with different length ratio: (a) 1:1; (b) 2:1; (c) 3:1 and (d) 4:1. All alumina nanochannels have nearly the same length about 45 μm . (e) I-V curves of the funnel-shaped alumina nanochannels with different length ratio.

In our work, the ion selective behavior of the funnel-shaped alumina nanochannels with different length ratio was investigated. As shown in Figure 2S (a-d), alumina nanochannels with different length ratio was prepared by controlling the anodization time. From Figure S2a to S2d, the anodization time for the growth of the taper nanochannels was about 9.6 h, 9 h, 8 h and 6 h, respectively. The length of the funnel-shaped nanochannels is controlled about 45 μm due to a total of anodic oxidation time was about 12 h. Figure S2e shows the nonlinear I-V curves of the funnel-shaped alumina nanochannels with different length ratios. This ion selective transportation in asymmetric nanochannels can be explained by the ratchet model¹. The concentration of ions at neck nanochannels increases, which results in a ratchet potential assisted by the structural asymmetry. When a positive voltage is applied, the

ions flow from the taper nanochannel to the neck nanochannel. The electrostatic traps formed by the ratchet potential inhibit the ion transport through the funnel nanochannels. At a negative voltage, the electrostatic traps are not formed. The high concentration of ions on the neck nanochannels enhances the ionic current. With adjusting the length ratios from 1:1 to 4:1, the high conductance and ion selective transportation has been exhibited. The increase of the length ratios of two segments of nanochannels was equal to enhance the asymmetry of the nanochannels, which resulted in a noticeable ratchet potential ². Therefore, the funnel-shaped alumina nanochannels with length ratio of 4:1 were chosen as the candidate for sensing metal ions.

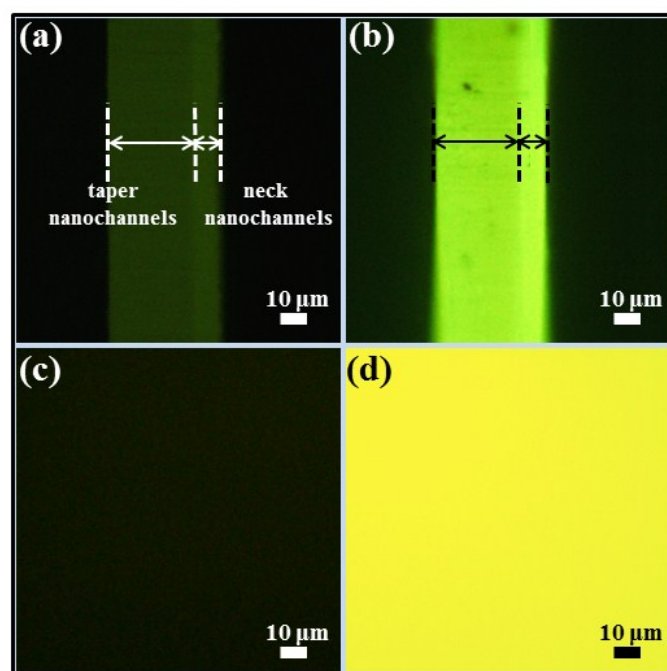


Figure S3. Fluorescent images of the alumina nanochannels: the fluorescent micrographs of the cross-section (a) before and (b) after modifying with ssDNA; the fluorescent micrographs of the neck nanochannels opening side (c) before and (d)

after grafting ssDNA.

The fluorescent micrographs of the naked and modified ssDNA alumina nanochannels were investigated by a fluorescent microscope (Vision Engineering Co., UK). As shown in Figure S3, the strong fluorescent signal of the cross-section was observed after modifying ssDNA. Moreover, both the neck and the taper nanochannels exhibited a strong fluorescent signal after modifying ssDNA, indicating the uniform modification of the ssDNA on the interior surface of the alumina nanochannels. The fluorescent signal of the neck nanochannels opening side was observed after grafting ssDNA.

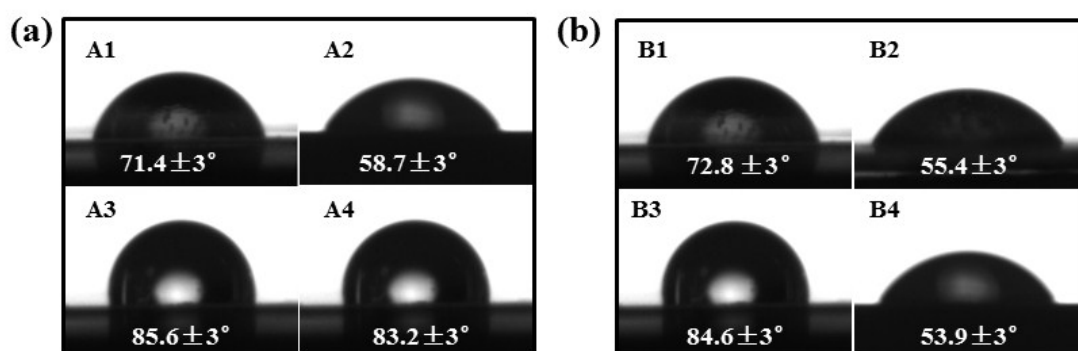


Figure S4. Wettability changes of the ssDNA-modified alumina nanochannels which respond to (a) Hg²⁺ and (b) Ag⁺ ions respectively: (A1 and B1) the naked alumina nanochannels; (A2 and B2) the alumina nanochannels modified with ssDNA; respond to Hg²⁺ and Ag⁺ ions at the neutral pH (A3 and B3) and pH 4.5 (A4 and B4).

In order to confirm the successful of the ssDNA modification and the conformation change on the interior surface of the alumina nanochannels, the contact angle measurement was investigated (Figure S4). The contact angle was measured

using an OCA20 machine (DataPhysics, Germany) contact-angle system. In each measurement, 2 μL droplet of water was dispensed onto the neck nanochannels side. The contact angle decreased after immobilizing ssDNA (A2 and B2), providing an evidence of the successful modification. After the ssDNA interacting with Hg^{2+} or Ag^+ ions, it would increase the contact angle of the alumina nanochannels (A3 and B3). When the pH value changed to 4.5, the contact angle of the alumina nanochannels which responds to Hg^{2+} ions (A4) was almost unchanged, while the contact angle which respond to Ag^+ ions (B4) was drastically reduced as a result of the conformational transformed from the C- Ag^+ -C duplex structures to the “i-motif” quadruplex structures.

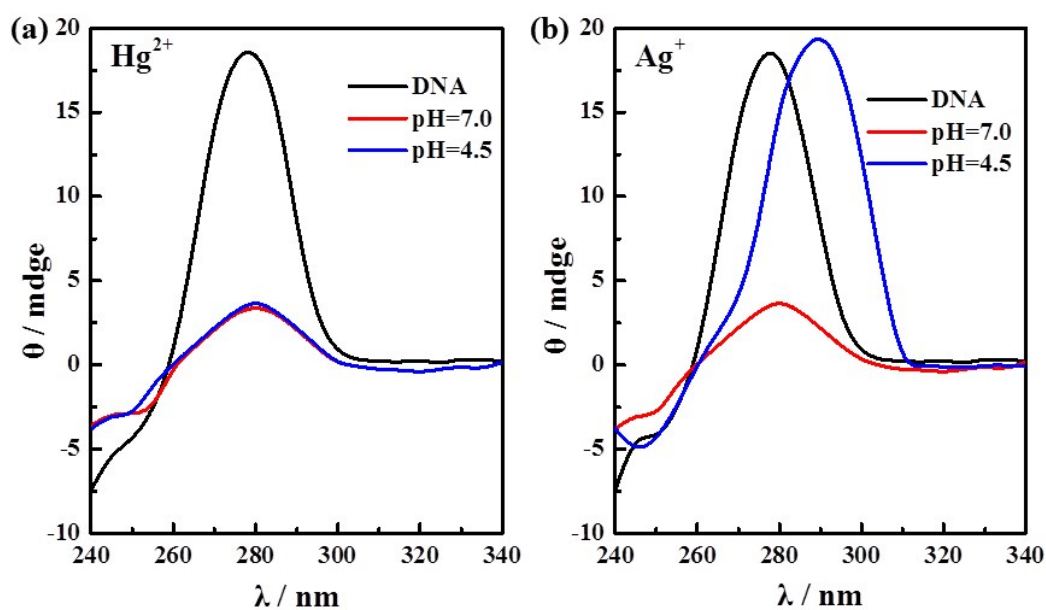


Figure S5. Conformational switch of the responsive ssDNA interacted with (a) Hg^{2+} and (b) Ag^+ ions by the CD measurement.

The conformational change of the ssDNA was also determined by CD spectra measurements. The wavelength scans were performed between 240 and 340 nm. As

shown in Figure. S5, when the ssDNA Tris-HCl buffer solution was in contact with Hg^{2+} or Ag^+ ions at pH 7.0, the characteristic peak at 280 nm (the red curve) of the ssDNA was almost disappeared, indicating a typical T- Hg^{2+} -T or C- Ag^+ -C conformation. No changes in the CD spectra could be observed after changing the pH value of Hg^{2+} ions solution to 4.5 (blue curve in Figure S5a), while there was a red-shifted for Ag^+ ions at pH 4.5 (blue curve in Figure S5b).

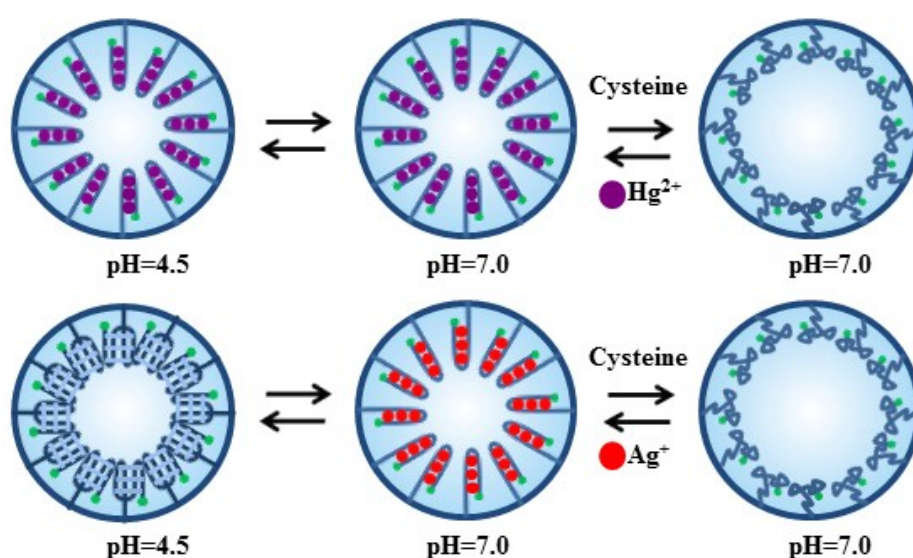


Figure S6. Conformation changes description in the interior of the funnel-shaped alumina nanochannels which modified with ssDNA: the ssDNA respond to Hg^{2+} ions kept double strand structure at both pH 4.5 and 7.0; a duplex-quadruplex reversible conversion can be triggered by decreasing the pH value when respond to Ag^+ ions; both Hg^{2+} and Ag^+ ions can be pulled out from the double strand complex by cysteine.

As shown in Figure S6, the ssDNA interacted with Hg^{2+} ions still maintained the T- Hg^{2+} -T structures at both pH 4.5 and 7.0, while the ssDNA which respond to Ag^+ ions underwent a conformational change between a double-stranded structure (at pH 7.0)

and a four-stranded i-motif structure (at pH 4.5). The responsive T-/C-rich ssDNA which interacted with Hg^{2+} and Ag^+ ions could be recovered by the thiol group cysteine, due to the tight binding interactions between cysteine and the metal ions.

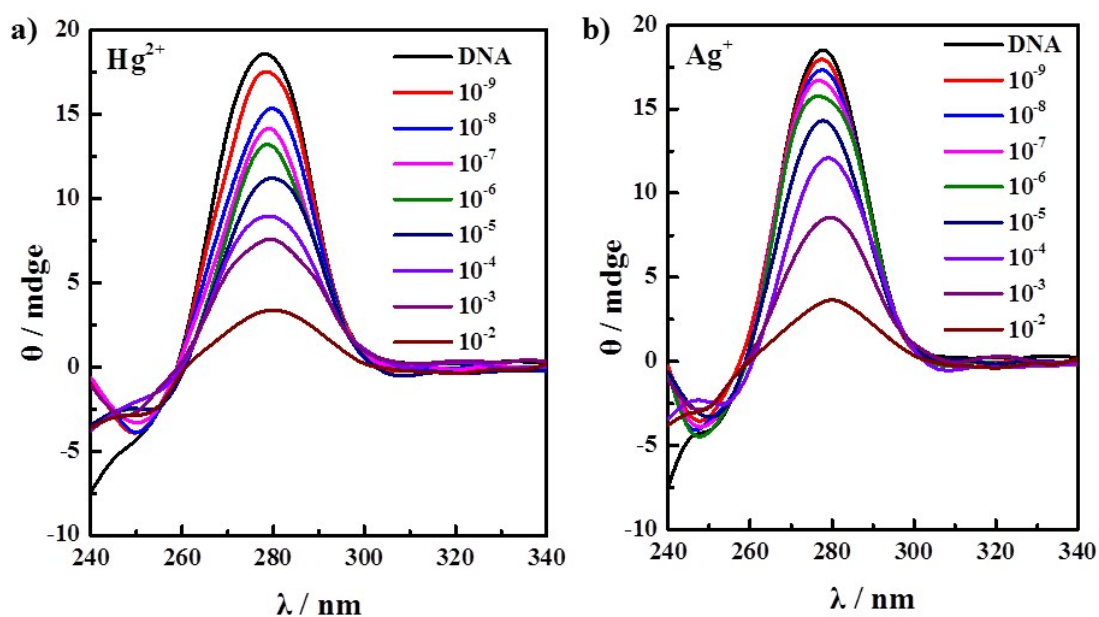


Figure S7. The CD spectra of the ssDNA in the presence of different concentration of (a) Hg^{2+} and (b) Ag^+ ions in Tris-HCl buffer solution.

As shown in Figure S7a, when concentration of Hg^{2+} ions increased from 0 to 10^{-2} M, the positive peak near 280 nm of ssDNA was slowly weakened because of the formation of T- Hg^{2+} -T complexes. As for Ag^+ ions, the similar CD signal changes were presented in Figure S7b.

References

1. Siwy, Z.S., *Adv. Funct. Mater.*, **2006**, 16, 6, 735-746.
2. P. Ramírez, P. A. Apel, J. Cervera, S. Mafé, *Nanotechnology*, **2008**, 19, 315707.